Eur J Plant Pathol (2020) 156:751–766
https://doi.org/10.1007/s10658-019-01926-5

# Phylogenetic and population genetic analyses reveal three distinct lineages of the invasive brown root-rot pathogen, *Phellinus noxius*, and bioclimatic modeling predicts differences in associated climate niches

**J. E. Stewart · M.-S. Kim · Y. Ota · N. Sahashi · J. W. Hanna · M. Akiba · J. P. Ata · N. Atibalentja · F. Brooks · C.-L. Chung · E. K. Dann · A. Mohd Farid · T. Hattori · S. S. Lee · K. Otto · G. S. Pegg · R. L. Schlub · L. S. Shuey · A. M. C. Tang · J.-N. Tsai · P. G. Cannon · N. B. Klopfenstein**

Accepted: 25 December 2019 / Published online: 30 January 2020


**Abstract** *Phellinus noxius,* the cause of brown root-rot disease, is an invasive fungal pathogen that causes a white rot among woody plants in Asia, Oceania, and Africa. Because the origin and diversity of this pathogen are unknown, it is difficult to predict its behavior and invasive capacity, especially under future climate-change scenarios. We characterized genetic relationships and ecological differences among *P. noxius* lineages across eastern Asia and Oceania to better understand evolutionary responses of the pathogen to environmental changes. Sequences of four loci (nuclear large subunit, internal transcribed spacers, partial RNA polymerase II, and partial translation elongation factor – 1 alpha) from 95 *P. noxius* isolates were used for genetic analyses. Our analyses revealed three genetically distinct lineages of *P. noxius*: 1) eastern Asia (Japan, Taiwan, Hong Kong, and Malaysia); 2) western Oceania/Japan/Taiwan (including Australia, Palau, Guam,

**Electronic supplementary material** The online version of this article (https://doi.org/10.1007/s10658-019-01926-5) contains supplementary material, which is available to authorized users.

J. E. Stewart (✉) · J. P. Ata · K. Otto
Department of Agricultural Biology, Colorado State University, Fort Collins, CO 80523, USA
e-mail: Jane.Stewart@colostate.edu

M.-S. Kim (✉)
USDA Forest Service, Pacific Northwest Research Station, Corvallis, OR 97331, USA
e-mail: meesook.kim@usda.gov

Y. Ota
Department of Forest Science and Resources, Nihon University, Fujisawa, Kanagawa 252-0880, Japan

N. Sahashi · M. Akiba · T. Hattori
Forestry and Forest Products Research Institute, Tsukuba, Ibaraki 305-8687, Japan

J. W. Hanna · N. B. Klopfenstein
USDA Forest Service, Rocky Mountain Research Station, Moscow, ID 83843, USA

N. Atibalentja
American Samoa Community College-CNR, Division of Community & Natural Resources, Pago Pago, AS 96799, USA

F. Brooks
1961 Westwood Pl., Pomona 91768 California, USA

C.-L. Chung
Department of Plant Pathology and Microbiology, National Taiwan University, Taipei City 10617, Taiwan

E. K. Dann
Queensland Alliance for Agriculture and Food Innovation, The University of Queensland, Brisbane, Australia

Saipan, Yap, Pohnpei, and Kosrae) with some isolates from Japan and Taiwan; and 3) a distinct group from American Samoa. Population genetic analyses highlighted admixture and migration among the three lineages. Climate-based, species distribution models were used to predict ecological patterns of *P. noxius* for two genetic lineages: eastern Asia and western Oceania/Japan/Taiwan. Contemporary bioclimatic models depicted potential areas at high risk for *P. noxius* invasion, and predicted that suitable climate space (potential distribution) is lineage specific. Trade of important economic crops worldwide coupled with changing climates could exacerbate the spread of *P. noxius* into new geographic areas with suitable habitats for brown root-rot disease.

**Keywords** Genetic lineages · Invasive forest pathogen · Species distribution model · Brown root rot disease · White rot

## Introduction

Threats by invasive fungal pathogens are increasing as globalization and changing climates interact around the globe (Fischer et al. 2012). Growing international commerce has significantly amplified threats from invasive pathogens (Leibhold et al. 2012). Warming global temperatures, along with changes in moisture regimes and seasonality, make it increasingly difficult to predict the likelihood for introduced pathogens to become established and result in disease emergence. Further, established dispersal pathways may facilitate the movement of invasive pathogens as environments become more suitable for the invasive pathogens over time (Chakroaborty 2013).

Understanding the biology of introduced pathogens is vital to predict how they will behave/respond as an invasive in naive environments. More specifically, understanding the genetic diversity, reproductive cycles, and phenotypic variations that occur within populations is critical for managing invasive species and helping prevent introductions to new areas. Previous studies have shown that invasiveness increases with increasing genetic and phenotypic variation (e.g., Forsman 2014). Commonly, genetic diversity is reduced in introduced populations compared to their native populations, which is known as the "founder effect" (Dean and Ballard 2004). Assessments of genetic diversity within introduced populations can uncover the number of genotypes, which can help identify invasion routes and implement measures to limit the introduction of more genotypes (Grünwald and Goss 2011). Multiple introductions can also enhance the invasiveness of a pathogen, because different genotypes may also differ phenotypically, in host preference, virulence, optimal temperature for growth/reproduction, and other adaptive capacities. Further, sexual reproduction among genotypes in an introduced population can also increase genetic diversity, invasiveness, and adaptive capacity (Desperez-Loustau et al. 2007). Similarly, diverse genotypes can hybridize or form unique combinations, potentially giving rise to novel pathogens (Dlugosch and Parker 2008). Two fungal species, *Ophiostoma ulmi* and *O. novo-ulmi*, causal agents of Dutch elm disease, were both introduced into the United States and Europe. Though closely related, they differ in many phenotypic traits, including temperature range for growth and aggressiveness to American and European elms, *Ulmus americana* and *U. laevis*, respectively. Apparently, interspecific hybridization, gene introgression, and sexual recombination generated evolutionary changes and higher genotypic diversity in *O. novo-ulmi*, which led to increased invasiveness (Brasier 2001).

*Phellinus noxius* (Corner) G. H. Cunningham is an invasive, tree-root pathogen that is destructive, fast-

A. Mohd Farid
Forest Health and Conservation Programme, Forest Research Institute Malaysia, Selango, 52109 Kepong, Malaysia

S. S. Lee
Tanarimba, Janda Baik,, 28750 Bentong, Pahang, Malaysia

G. S. Pegg · L. S. Shuey
Department of Agriculture and Fisheries, Queensland Government, Brisbane, Australia

R. L. Schlub
Cooperative Extension and Outreach, University of Guam, Mangilao, Guam 96923, USA

A. M. C. Tang
Muni Arborist Limited, Kowloon, Hong Kong, SAR, China

J.-N. Tsai
Plant Pathology Division, Taiwan Agricultural Research Institute, Taichung City 41362, Taiwan

P. G. Cannon
USDA Forest Service – Forest Health Protection, Region 5, Vallejo, CA 94592, USA

growing, and affects a wide range of woody hosts in pan-tropical areas, including Asia, Oceania, and Africa (e.g., Ann et al. 2002; Brooks 2002a, b). The fungus was first identified in Singapore in 1932 by Corner as *Fomes noxius* (Corner 1932). It was reclassified in 1965 as *Phellinus noxius* (Cunningham 1965). Although *P. noxius* causes a disease known as brown root rot, it is a white-rot fungus, able to degrade lignin, as well as cellulose and hemicellulose. Its hosts include breadfruit (*Artocarpus altilis*), Polynesian ironwood (*Casuarina equisetifolia*), mango (*Mangifera indica*), cacao (*Theobroma cacao*), coffee (*Coffea* spp.), and rubber (*Hevea brasiliensis*), as well as diverse fruit, nut, ornamental, and other native/exotic trees, with little host specificity (Farr and Rossman 2019). Symptoms of *P. noxius* infection can include reduced tree growth, defoliation, and branch dieback. This fungus can also survive as a saprophyte by colonizing the heartwood and other organic matter; it also can survive for up to 10 years within woody debris in the soil (Chang 1996). Brown root-rot disease can develop over several years, or in some cases, it can cause tree mortality within a year. In the 1980s, it was hypothesized that *P. noxius* was introduced into Northern Mariana Islands in the Pacific Ocean through infested wood or infected plants that arrived at the airport (Hodges and Tenorio 1984); however, genetic tools were unavailable at the time to investigate this hypothesis. Recent studies have examined the population genetics of *P. noxius* in Japan and Taiwan with microsatellites and genome-wide, single-nucleotide polymorphisms (Akiba et al. 2015; Chung et al. 2015; Chung et al. 2017). All of these studies found high levels of genetic diversity within populations. In Taiwan, Chung et al. (2015) suggested that the spread of *P. noxius* could occur either through mycelial growth within the soil, resulting in slow, localized spread of single genotypes, or through basidiospore spread, which can establish multiple genotypes over longer distances. In Japan, two distinct populations, with little admixture, were observed on the Ryukyu and Ogasawara Island chains. This suggested the possible invasion of a genetically distinct population to the Ogasawara Islands, possibly introduced via basidiospores or mycelium in wood carried by a typhoon from the Mariana Islands (Akiba et al. 2015). Further, the population found on the island of Ryukyu was also found in Taiwan (Chung et al. 2017). To understand the invasiveness of *P. noxius*, previous research suggests that it is important to identify its existing genetic diversity and any associated phenotypic traits (Bickford et al. 2007).

The global genetic diversity of *P. noxius* has yet to be studied, therefore it remains if *P. noxius* is a native or introduced species in tropical and sub-troptical regions where it is found. Furthermore, it is undetermined if distinct populations or cryptic species exist in diverse global regions. The focus of our study is to better understand the evolutionary history, worldwide movement, and potential ecological differences among genetically distinct lineages of *P. noxius* from geographically diverse sources. This research aims to further develop management strategies by assessing genetic relationships of *P. noxius* in eastern Asia and Oceania and predicting areas at high risk for invasion by genetic lineages of *P. noxius*.

## Materials and methods

### Isolates, PCR, and DNA sequencing

A total of 95 isolates was included in this study: Japan (4), Taiwan (8), Hong Kong (8), Malaysia (14), Australia (18), and the Pacific Islands of Palau (4), Guam (12), Saipan (4), Yap (4), Pohnpei (5), Kosrae (2), and American Samoa (12) (Suppl. Table 1; Fig. 1). Further, isolates were collected from a wide diversity of tropical host species (Suppl. Table 1). In preparation for DNA extraction, cultures were grown on a 0.2-μm pore, nylon filters (Millipore Corp., Billerica, MA, USA) overlaying potato dextrose agar for 7 days in the dark at 25 °C. Mycelia (ca. 100 mg) were scraped from the filter and ground in extraction buffer using a FastPrep®_ FP120 cell disruptor (Qbiogene, Carlsbad, CA, USA) and ZR Fungal/Bacterial DNA MiniPreps (Zymo Research Corporation, Irvine, CA, USA). Extractions were performed following manufacturer's protocols with minor modifications. DNA quantity and quality were estimated using a NanoDrop™ 2000 (Thermo Fisher Scientific, Wilmington, DE, USA).

For each isolate, sequencing was performed on four loci [28S (nuclear large subunit; LSU) region of rDNA, internal transcribed spacers 1 and 2 with 5.8S regions of rDNA (ITS); partial translation elongation factor – 1 alpha (*tef1*); and partial RNA polymerase II, second largest subunit (*rpb2*)], which was similar to previous work by Brazee and Lindner (2013) on the *Phellinus* s.*l.* complex in North America. Primer sets for

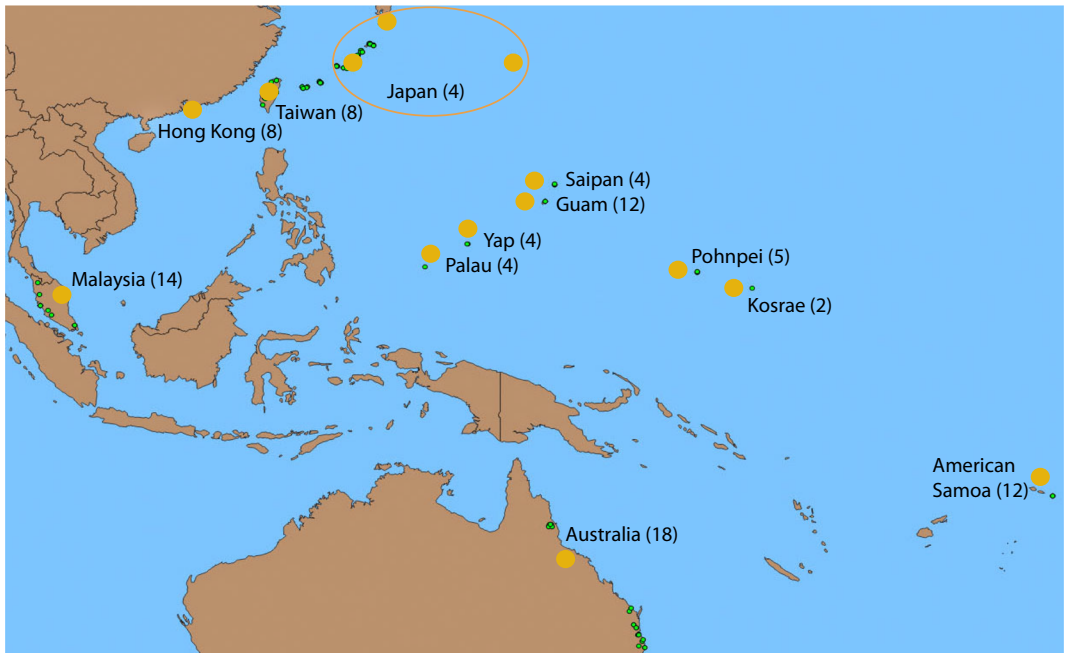


**Fig. 1** GPS locations of *Phellinus noxius* isolates collected in eastern Asia, western Oceania, and American Samoa. Yellow and green circles indicate where isolates of *P. noxius* were collected for this study. Numbers in parenthesis indicate the number of isolates from each region

amplification included 1) LR0R (Rehner and Samuels 1994) and LR5 (Vilgalys and Hester 1990) for LSU domains one to three; 2) ITS1 and ITS4 (White et al. 1990) for the ITS; 3) 983F and 2218R for the *tef1* (Rehner and Buckley 2005); and 4) bRPB2-6F and bRPB2–7.1R (Matheny 2005) for the *rbp2*. Amplification reaction mixtures (total 25 μl) contained 20–40 ng of template DNA, 2.5 μl 10x Standard *Taq* Reaction Buffer (New England BioLabs Inc., USA), 0.5 μl 10-mM dNTPs (Roche Applied Science, USA), 1 μl each of 10-μM primer and 1.25 U *Taq* DNA Polymerase (New England BioLabs Inc.). Amplifications were performed using the following PCR conditions: 94 °C for 1 min, 35 cycles at 95 °C for 30 s, 55–58 °C (depending on primers: 58 °C for LSU, 58 °C for ITS, 55 °C for *tef1*, and 55 °C for *rpb2*) for 30 s, and 72 °C for 45 s, and finally 72 °C for 10 min. All PCR reactions were conducted using an MJ PTC-200 thermocycler (Bio-Rad Laboratories, Waltham, MA, USA). PCR products were electrophoresed in 1.5% agarose gels with 0.5X TBE buffer and stained with GelRed® (Biotium, Fremont, CA, USA) and bands were visualized using UV light. PCR products were treated with ExoSAP-IT® PCR Product Cleanup (Affymetrix, Santa Clara, CA, USA) following manufactures instructions. Sequencing was performed with the Big Dye Sequencing Kit v. 3.1 on an ABI 3130xl capillary sequencer (Applied Biosystems, Foster City, CA, USA) at Eurofins MWG Operon USA (Louisville, KY, USA).

## Phylogenetic and parsimony network analyses

Sequences were visualized with Geneious v. 9 (Kearse et al. 2012) and aligned with MUSCLE (Edgar 2004). Genotype sequences were phased into haplotypes for each locus in DnaSP v.5 (Rozas et al. 2003). Alignment files are housed in TreeBase under accession # 23998. Phased data, of the combined dataset and for each locus, were used to estimate the number of unique haplotypes, segregating sites, pairwise nucleotide diversity ($\pi$), Watterson's theta, Tajima's *D* (Tajima 1989) test for neutrality and putative minimum number of recombination events. These analyses were performed for the three identified lineages 1) eastern Asia (Japan, Taiwan, Hong Kong, and Malaysia), 2) western Oceania (Australia, Palau, Guam, Saipan, Yap, Pohnpei, and Kosrae with selected genotypes from Japan and Taiwan, but excluding American Samoa; hereafter referred to as "western Oceania/Japan/Taiwan"), and 3) American Samoa. These lineages were estimated using the phylogeny of

*tef1* locus. Haplotype networks were constructed for the ITS and *rpb2* using statistical parsimony implemented in TCS v1.21 using a 92% similarity cutoff (Clement et al. 2000). A network was not completed for the *tef1* locus because the genetic distance among all sequences was greater than the minimum 90% as implemented in TCS.

Phylogenies for the LSU, ITS, and *tef1* were inferred for collapsed haplotypes with Bayesian inference and likelihood methods using BEAST (Drummond et al. 2012) and PhyML (Guindon et al. 2010), respectively. DT-ModSel (Minin et al. 2003) was used to estimate the best-fit, nucleotide-substitution models for each dataset. Bayesian inference was performed with parameter settings suggested by the best-fit, nucleotide-substitution models. Data sets were run for 50 million generations with sampling every 5000 generations. Analyses were performed three times. Log files and ESS values were evaluated in TRACER version 1.5 (Heled and Drummond 2010), and consensus trees were calculated using TreeAnnotator v1.7.2 with a burn-in of 5000 trees. FigTree v1.3.1 (Rambaut 2009) was used to visualize the consensus tree node ages, branch lengths and posterior probabilities.

### Genetic distance and differentiation

Genetic distances among each of the geographic origins (e.g., country, region, or island) were estimated using DnaSP (Rozas et al. 2003) using the concatenated dataset. Two measures of genetic differentiation, $F_{ST}$ and $K_{ST}$* (Hudson et al. 1992a; Hudson et al. 1992b) were used to determine if populations were structured by geographic origin (Japan, Taiwan, Malaysia, Hong Kong, Australia, Palau, Guam, Saipan, Yap, Pohnpei, and American Samoa), with the exception of Kosrae for which the sample size was insufficient for analyses. $F_{ST}$, as presented in Hudson et al. (1992b), is an estimate of the average divergence between pairs of sequences within subpopulations and average divergence between pairs of sequences randomly drawn from the whole population. $K_{ST}$* is estimated by determining the proportion of genetic diversity within populations compared to the diversity in the total population (Hudson et al. 1992a). Significance for $K_{ST}$* was estimated by 1000 permutations of the data as implemented in DnaSP v5.

### Bioclimatic modeling

Climate-based, species-distribution models using MaxEnt v3.3.3 K (Maximum Entropy Species Distribution Modeling) were created for three data sets. These consisted of a model using 179 locations of DNA-sequence confirmed occurrence records that were associated with a precise GPS location (Suppl. Table 2) and two reduced sets based on eastern Asia (Fig. 6c, N = 26) and western Oceania/Japan/Taiwan (Fig. 6d, N = 44) genetic groups. The American Samoa population was not included in the reduced set analyses because of limited geographic diversity among occurrence points. MaxEnt was used because of its ability to produce statistically sound models with presence-only data and relatively limited occurrence data (Elith et al. 2006, 2011). The models used 19 bioclimatic variables (e.g., annual mean temperature, maximum temperature of warmest month, annual precipitation, precipitation of wettest month, precipitation of coldest quarter, etc.) in a set of high-resolution (30 arc sec, ca. 1-km$^2$) interpolation grids based on contemporary climate from 1979 to 2013 [CHELSA data (climatologies at high resolution for the earth's land surface areas data), http://chelsa-climate.org, Karger et al. 2017]. MaxEnt settings included random subsample sets (25%) to generate statistical results among 15 replicate runs. Quantum GIS (QGIS; http://www.qgis.org/en/site/) was used to create the final outputs using MaxEnt's cumulative output. Each cumulative value is the sum of probabilities of cells less than or equal to the cell grid, times 100. MaxEnt's cumulative output was chosen for easier conceptualization compared to MaxEnt's logistic (an index of probability from 0 to 1) or raw exponential output.

## Results

### Phylogenetic lineages

The LSU and ITS Bayesian phylogenies highlighted a general grouping of *P. noxius* sequences, while showing that the genus *Phellinus* is polyphyletic (Figs. 2 and 3). With LSU, isolates collected in this study grouped within a well-supported clade with *P. noxius* s.l. LCO66633, which was distinct from a well-supported clade containing *Pyrrhoderma noxium* sequences (Fig. 2). However, with ITS, the 66 haplotypes collected in this study formed

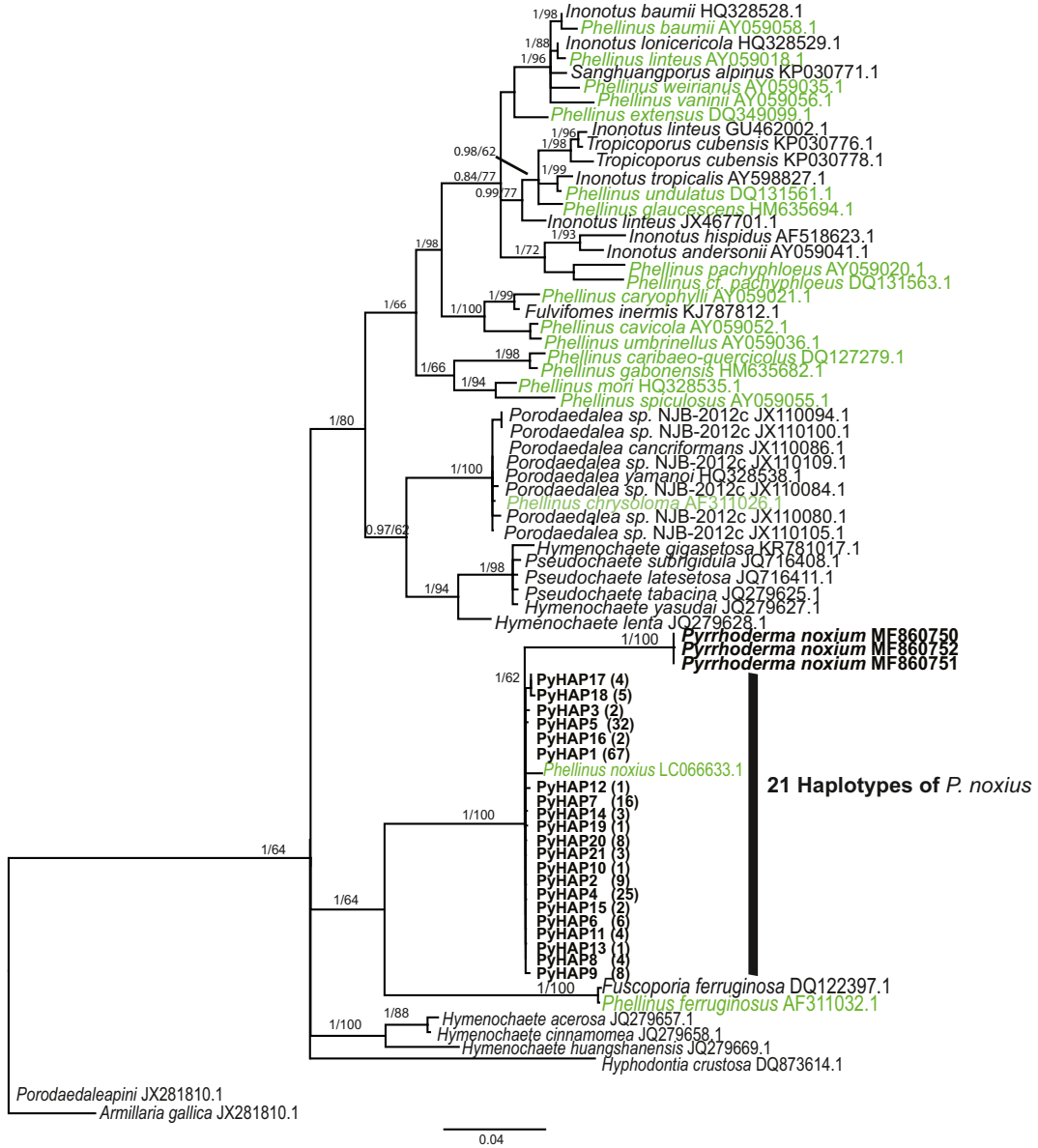


**Fig. 2** The nuclear large subunit (LSU) Bayesian phylogeny of *Phellinus* and other genera in *Phellinus sensu lato*. *Armillaria gallica* was chosen as an outgroup. Green text indicates *Phellinus* species, whereas bolded black text indicates *Pyrrhoderma noxium*. Haplotypes of *P. noxius* were used, and the number of isolates represented by each haplotype are placed next to the haplotype number. Numbers above each node indicate support (posterior probability/bootstrap)

a polytomy with some sequences attributed to *P. noxium* with clear separation from other *Phellinus* spp., including a distinct clade comprising other *P. noxium* sequences (Fig. 3). The *tef1* locus produced the highest phylogenetic signal of the four loci (Fig. 4). The Bayesian *tef1* phylogeny showed three distinct clades of *P. noxius* that primarily separated sequences associated with general geographic regions. All sequenced isolates from Hong Kong and Malaysia grouped with high posterior probability support (PP = 1.00) into an eastern Asia clade, which also contained some isolates from Japan and Taiwan. The American Samoa clade, which included all 12 isolates from American Samoa, formed a separate clade with PP and bootstrap (BS) support of 1.00 and 62, respectively. This clade was more closely related to isolates from Australia, Palau, Guam, Saipan, Yap, Pohnpei,

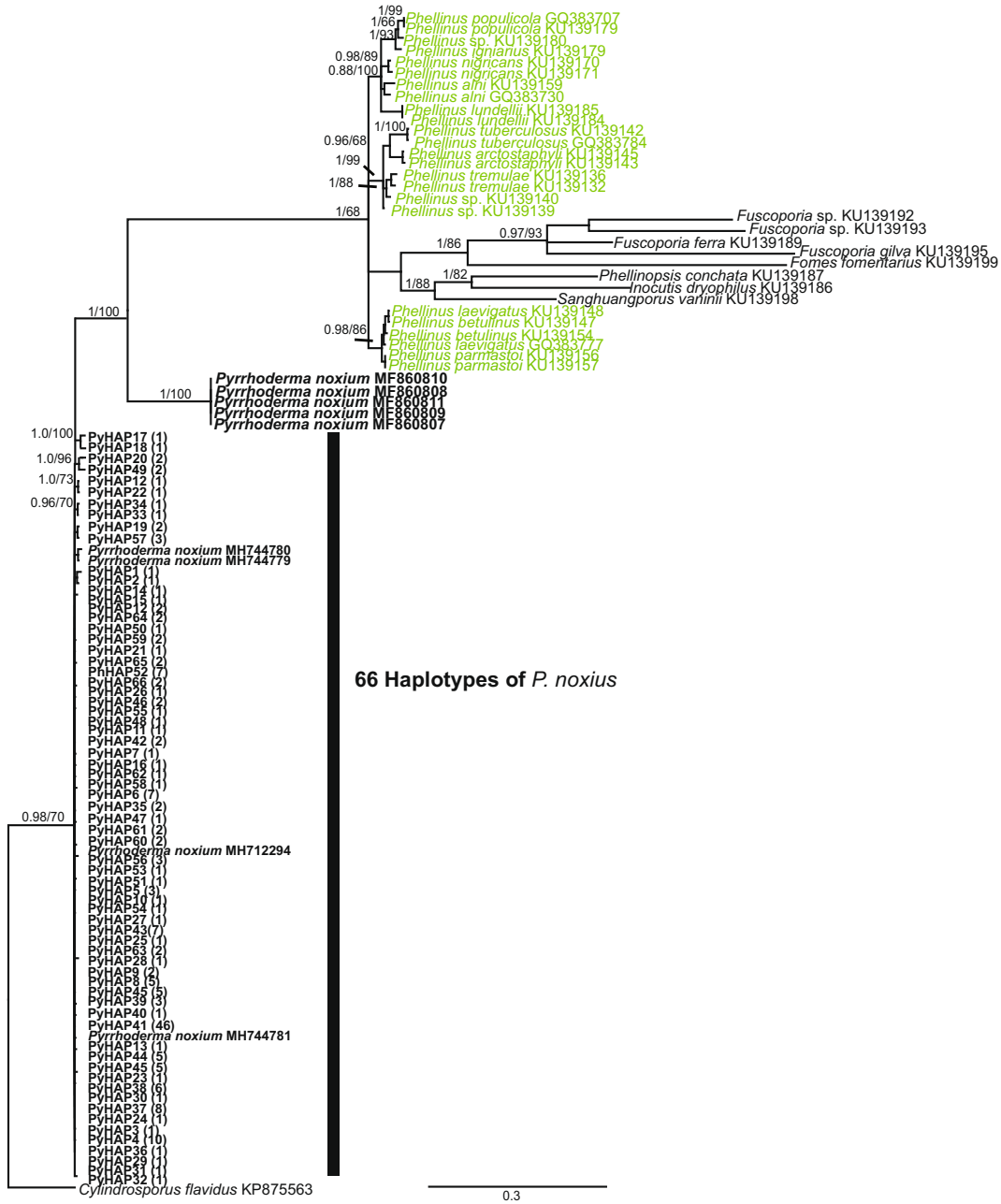


**Fig. 3** The internal transcribed spacers 1 and 2 with 5.8S regions of rDNA (ITS) Bayesian phylogeny of *Phellinus*, and other genera in *Phellinus sensu lato, with Cylindrosporus flavidus* serving as the outgroup. Green text indicates *Phellinus* species, and sequences from other genera (*Fuscoporia*, *Fomes*, *Phellinopsis*, *Inocutis*, and *Sanghuangporus*) were included for comparative purposes. Bolded black text indicates *Pyrrhoderma noxium* and *Phellinus noxius*. Haplotypes of *P. noxius* were used, and the number of isolates represented by each haplotype are placed next to the haplotype number. Numbers above each node indicate support (posterior probability/bootstrap)

and Kosrae that grouped in a third distinct lineage. This western Oceania/Japan/Taiwan clade also contained some isolates from Japan and Taiwan, but no isolates from American Samoa. Isolates from Australia, along with some isolates from Palau, Yap, and Pohnpei, formed a distinct monophyletic subclade (PP = 1.00; BS = 60) within in the western Oceania/Japan/Taiwan clade.

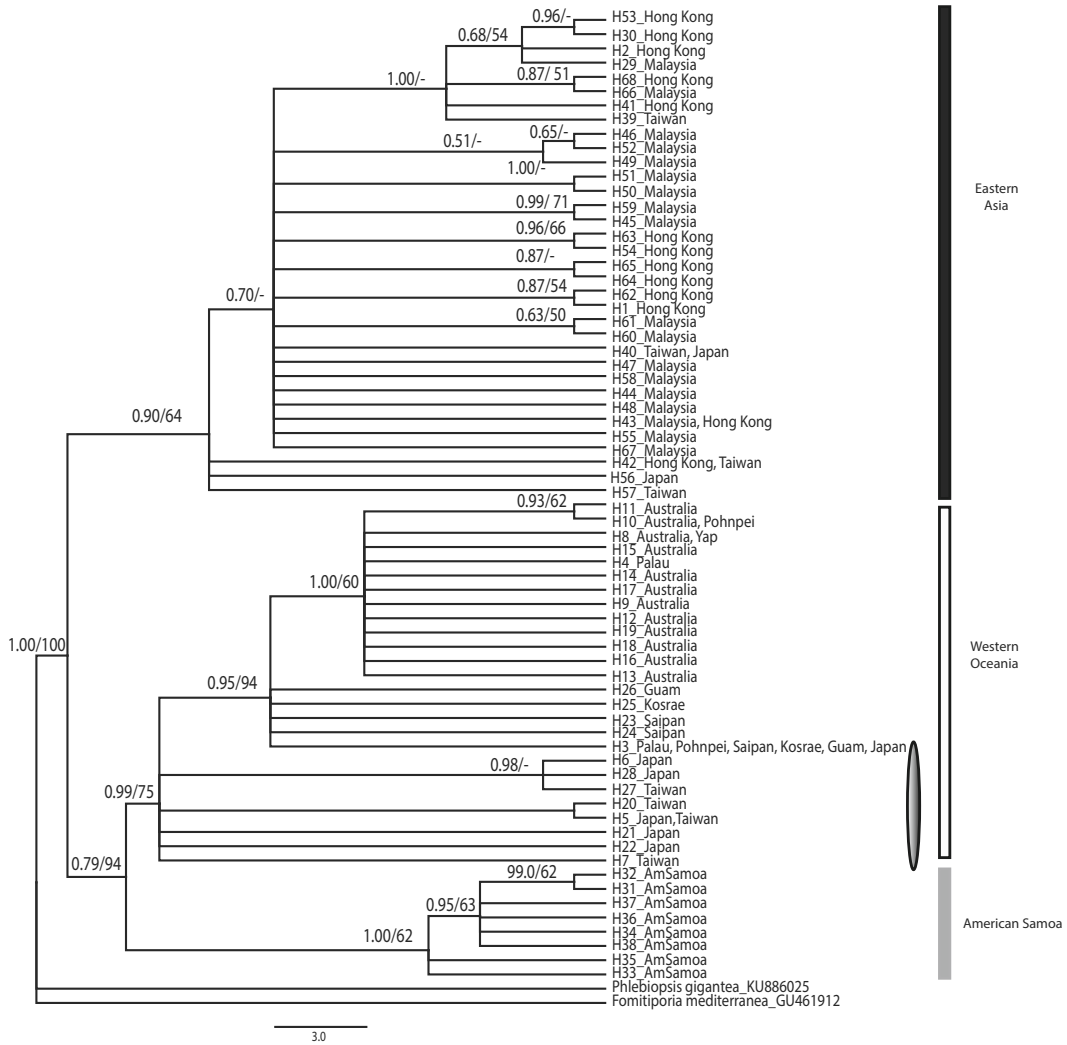


**Fig. 4** Bayesian inferred phylogeny for isolates of *Phellinus noxius* for partial translation elongation factor – 1 alpha (*tef1*). Phylogeny was rooted from *Phlebiopsis gigantea* and *Formitoporia mediterranea*. Numbers indicated node support (posterior probability/bootstrap). Bars highlight distinct clades: Black - Eastern Asia, White – western Oceania/Japan/Taiwan, Grey – American Samoa. The vertical oval depicts isolates from Japan and Taiwan that grouped with the western Oceania clade

## Haplotype networks

Parsimony haplotype networks of ITS and *rpb2* sequences from *P. noxius* also highlighted the existence of these two major phylogenetic groups (Fig. 5a, b). However, signals of admixture or migration were observed where isolates from the eastern Asia and western Oceania/Japan/Taiwan regions share haplotypes. At the *rpb2*, however, isolates from American Samoa formed a distinct group, but at the ITS, one American Samoa haplotype was shared with two isolates from Australia, and two haplotypes from Kosrae clustered with American Samoa isolates.

## Genetic diversity, neutrality, and recombination

A total of 3441 nucleotides were sequenced (LSU, 879 bp; ITS, 621 bp; *tef1*, 1081 bp; and *rpb2*, 860 bp)

**Fig. 5** Haplotype networks of Phellinus noxius constructed for internal transcribed spacers 1 and 2 with 5.8S regions of rDNA (ITS) (**a**) and partial RNA polymerase II, second largest subunit (rpb2) (**b**). Haplotypes are represented as circles proportional in size to the number of isolates in each haplotype. Inferred intermediate haplotypes are represented by a small, solid dot on the network. The number of isolates in each haplotype are proportionally represented in pie charts. Segments connecting the circles indicate the number of mutations separating the haplotypes.

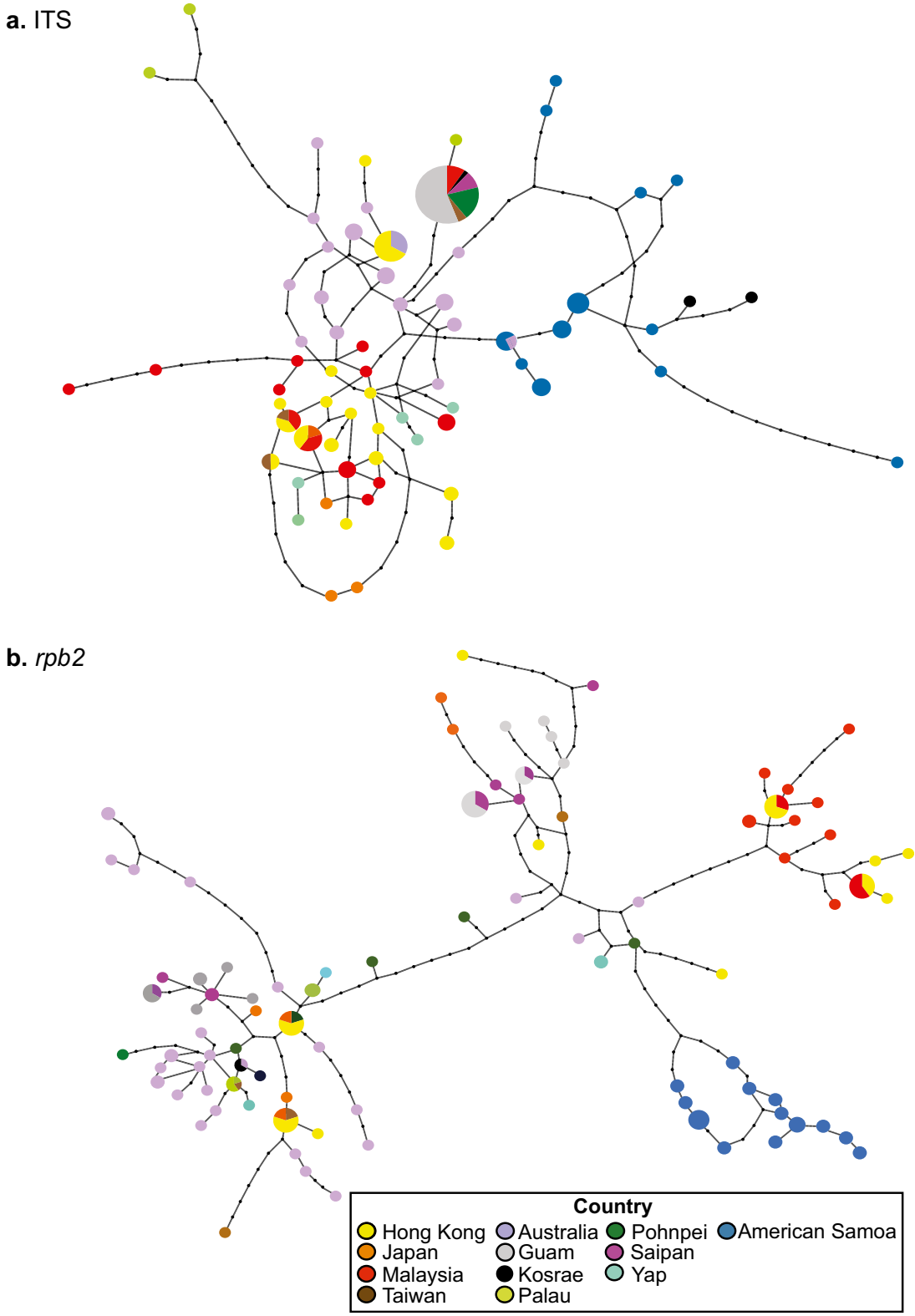
a. ITS
b. rpb2
Country
Hong Kong
Japan
Malaysia
Taiwan
Australia
Guam
Kosrae
Palau
Pohnpei
Saipan
Yap
American Samoa

**Table 1** Total number of sites, haplotypes, sequence diversity, segregating sites, and nucleotide diversity for each locus

| Locus (bp) | # phased isolates[a] | H [b] | Seg. sites [c] | H*d*[d] | ThetaW[e] | π [f] | Tajima's D[g] | Min Recom[h] |
|---|---|---|---|---|---|---|---|---|
| LSU (879) | | | | | | | | |
| Total | 190 | 21 | 10 | 0.842 | 0.0020 | 0.003 | 0.4311 | 2 |
| Eastern Asia | 60 | 12 | 7 | 0.845 | 0.0017 | 0.002 | 0.8609 | 3 |
| Western Oceania/Japan/Taiwan | 106 | 12 | 7 | 0.685 | 0.0012 | 0.001 | −0.4701 | 1 |
| American Samoa | 24 | 5 | 4 | 0.623 | 0.0012 | 0.001 | −0.3482 | 0 |
| ITS (621) | | | | | | | | |
| Total | 176 | 66 | 36 | 0.929 | 0.011 | 0.010 | −0.483 | 10 |
| Eastern Asia | 52 | 24 | 23 | 0.966 | 0.008 | 0.007 | −0.416 | 4 |
| Western Oceania/Japan/Taiwan | 100 | 33 | 27 | 0.814 | 0.009 | 0.008 | −0.810 | 6 |
| American Samoa | 24 | 14 | 15 | 0.928 | 0.007 | 0.008 | −0.836 | 5 |
| *tef*1 (1081) | | | | | | | | |
| Total | 190 | 68 | 87 | 0.926 | 0.014 | 0.008 | −1.372 | 9 |
| Eastern Asia | 60 | 39 | 59 | 0.981 | 0.011 | 0.007 | −1.372 | 6 |
| Western Oceania/Japan/Taiwan | 106 | 23 | 29 | 0.782 | 0.005 | 0.002 | −1.849* | 1 |
| American Samoa | 24 | 7 | 6 | 0.699 | 0.001 | 0.001 | −1.301 | 0 |
| *rpb*2 (860) | | | | | | | | |
| Total | 190 | 100 | 99 | 0.983 | 0.020 | 0.014 | −1.047 | 15 |
| Eastern Asia | 60 | 28 | 55 | 0.912 | 0.014 | 0.011 | −0.691 | 9 |
| Western Oceania/Japan/Taiwan | 106 | 63 | 60 | 0.980 | 0.013 | 0.011 | −0.721 | 13 |
| American Samoa | 24 | 11 | 13 | 0.895 | 0.004 | 0.005 | −1.202 | 2 |
| LSU + ITS + *tef*1 + *rpb*2 (3441) | | | | | | | | |
| Total | 190 | 154 | 196 | 0.997 | 0.012 | 0.008 | n/a | 28 |
| Eastern Asia | 60 | 47 | 121 | 0.989 | 0.009 | 0.007 | n/a | 20 |
| Western Oceania/Japan/Taiwan | 106 | 87 | 96 | 0.994 | 0.007 | 0.004 | n/a | 17 |
| American Samoa | 24 | 22 | 38 | 0.993 | 0.003 | 0.003 | n/a | 10 |

[a] All *Phellinus noxius* isolates were phased in to putative haploid genotypes in DnaSP (Rozas et al. 2003)

[b] Number of unique haplotypes out of total number of haploid genotypes in each population

[c] Number of segregating sites calculated in DnaSP

[d] Haplotype diversity calculated in DnaSP

[e] Watterson's theta calculated in DnaSP

[f] Nucleotide diversity calculated in DnaSP

[g] Tajima's *D* calculated in DnaSP. Values that significantly differ from neutrality ($P \leq 0.05$) based on 1000 permutations are indicated by an *

[h] Minimum number of recombination events calculated in DnaSP

with a total of 196 (5.7%) segregating sites among the multilocus dataset (Table 1). The most diverse locus was *rpb2* with a haplotype diversity (H*d*) = 0.983, nucleotide diversity ($\pi$) = 0.014, and Watterson's theta ($W_\theta$) = 0.020, compared to the other loci; LSU (H*d* = 0.842; $\pi$ = 0.003; $W_\theta$ = 0.0020), ITS (H*d* = 0.929; $\pi$ = 0.010; $W_\theta$ = 0.011), and *tef*1 (H*d* = 0.926; $\pi$ = 0.008; $W_\theta$ = 0.014) (Table 1). Evidence of neutrality was apparent as Tajima's *D* was non-significant for all loci (Table 1), which suggests that selection was not acting generally on these loci. Putative recombination events were evident within all loci (LSU, ITS, *tef1*, and *rpb2*) and the concatenated dataset across the entire isolate population and within separate lineages. For the LSU and *tef1* loci, no recombination was observed for the American Samoa lineage, though recombination was observed at the ITS and *rpb2* with MinRecom = 5 and 2, respectively. Putative recombination events within the western Oceania/Japan/Taiwan lineage ranged from one recombination event for *tef1* and LSU to 13

**Table 2** Pairwise $F_{ST}$ values for the MLST dataset for *Phellinus noxius* isolates grouped by region/area of origin

| | Japan | Taiwan | Hong Kong | Malaysia | Australia | Palau | Guam | Saipan | Yap | Pohnpei | American Samoa |
|---|---|---|---|---|---|---|---|---|---|---|---|
| Japan | – | | | | | | | | | | |
| Taiwan | 0.143* | – | | | | | | | | | |
| Hong Kong | 0.458* | 0.426* | – | | | | | | | | |
| Malaysia | 0.452* | 0.452* | 0.033* | – | | | | | | | |
| Australia | 0.219* | 0.301* | 0.658* | 0.669* | – | | | | | | |
| Palau | 0.234* | 0.183* | 0.609* | 0.628* | 0.243* | – | | | | | |
| Guam | 0.202* | 0.290* | 0.677* | 0.687* | 0.324* | 0.214* | – | | | | |
| Saipan | 0.216* | 0.297* | 0.426* | 0.674* | 0.364* | 0.294* | 0.016[ns] | – | | | |
| Yap | 0.279* | 0.363* | 0.721* | 0.732* | 0.183* | 0.292* | 0.459* | 0.508* | – | | |
| Pohnpei | 0.154* | 0.182* | 0.682* | 0.695* | 0.139* | 0.216* | 0.256* | 0.324* | 0.212* | – | |
| American Samoa | 0.467* | 0.483* | 0.702* | 0.708* | 0.613* | 0.598* | 0.726* | 0.736* | 0.766* | 0.699* | – |

$F^{ST}$ was not included for the Kosrae population because small sample size

*Using $K_{ST}$ to determine significant differentiation, all but one of the comparisons were significant ($P < .001$) indicating significant genetic differentiation

[ns] When comparing Saipan and Guam no significant genetic differentiation was observed ($K_{ST}$* = 0.0046; $P = 0.271$)

events for *rpb2*. In contrast, putative recombination events ranged from 9 within the *rpb2* to 3 at the LSU for the eastern Asia lineage (Table 1).

Though fewer isolates were contained within the eastern Asia lineage, it was the most diverged dataset at the *tef1* locus where $\pi = 0.007$ compared to 0.002 and 0.001 for the western Oceania/Japan/Taiwan and American Samoa lineages, respectively. At the *rpb2* locus, genetic diversity was similar between the eastern Asia and western Oceania/Japan/Taiwan lineages with $\pi = 0.011$ for both populations. At the LSU, *tef1*, and *rpb2* loci, the American Samoa lineage was the least diverse with $\pi$ ranging from 0.001 at LSU to 0.005 at *rpb2*. Interestingly, at the ITS locus, similar amounts of diversity were found across all three populations with $\pi$ ranging from 0.007 to 0.008.

Using the multi-locus nucleotide dataset, genetic differentiation among all geographic populations was estimated using pairwise comparisons of $F_{ST}$ and $K_{ST}$* (Table 2). Highest genetic differentiation was observed between the Malaysia population and populations from Australia, Palau, Guam, Saipan, Yap, Pohnpei, and American Samoa with $F_{ST}$ values of 0.669, 0.628, 0.687, 0.674, 0.732, 0.695, and 0.708, respectively (Table 2). High values of genetic differentiation were also observed between the American Samoa population and populations from Hong Kong, Malaysia, Guam, Saipan, Yap, and Pohnpei with $F_{ST}$ values ranging from 0.702, 0.708, 0.726, 0.736, 0.766, and 0.699, respectively. Genetic differentiation was smallest when comparing Hong Kong and Malaysia populations ($F_{ST} = 0.033$), and Guam and Saipan populations ($F_{ST} = 0.016$).

Highly significant genetic differentiation was detected when comparing all populations with a $K_{ST}$* = 0.252 ($P < 0.001$). Of the pairwise comparisons, all but one was significant, indicating genetic differentiation across geographic populations. When comparing Saipan and Guam, however, no significant differentiation ($F_{ST} = 0.016$) was observed with $K_{ST}$* = 0.0046 ($P = 0.271$).

## Bioclimatic modeling

Bioclimatic modeling analysis results for the all-locations model include an average AUC [Area Under the Receiver Operating Characteristics (ROC)] of 0.993 with a standard deviation of 0.001 over the 15 replicate runs (Fig. 6a, b). An AUC of 1 represents a model that perfectly fits all of the testing data while any value over 0.9 is considered to have 'excellent' performance (Araújo et al. 2005). Variables with the highest contribution to this model were Precipitation of Warmest Quarter (32.2%), Temperature Annual Range (13.6%), Precipitation Driest Month (13.1%), and Mean Diurnal Range (12.9%). A jackknife test of variable importance revealed that Mean Diurnal Range was the variable that provided the most useful information, independently (highest training gain),

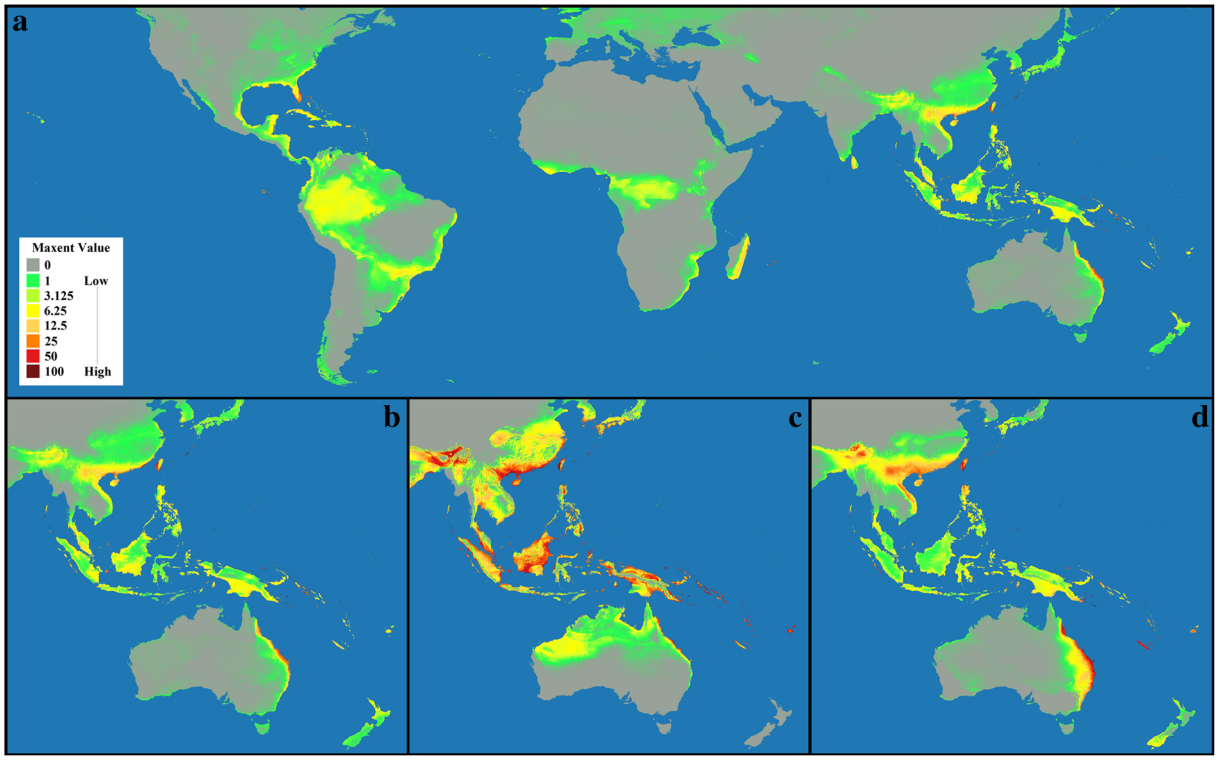


**Fig. 6** Maxent bioclimatic predictions of potential distribution (suitable climate space) for *Phellinus noxius* (6a, global and 6b, regional) based on all DNA confirmed records of occurrence; and regional models: 6c = Eastern Asia (Group 1), and 6d = western Oceania/Japan/Taiwan (Group 2). Color shades ranging from green to red represent increasing Maxent values (probability) of suitable climate space (climate niches) for *P. noxius*

while Precipitation of Warmest Quarter provided the most useful information that was not represented in other variables (i.e., caused the largest decreases in gain when omitted). The Eastern Asia (Group 1) model had an AUC of 0.998 with a standard deviation of 0.002 (Fig. 6c). The variables with the highest contributions were Precipitation Warmest Quarter (25.5%), Mean Diurnal Range (24.2%), Mean Temperature Warmest Quarter (12.4%), and Precipitation Wettest Quarter (10.7%). The jackknife test revealed Precipitation Warmest Quarter had the highest training gain and also the largest decreases in gain when omitted. Lastly, the western Oceania/Japan/Taiwan (Group 2) model had an AUC of 0.997 with a standard deviation of 0.001 (Fig. 6d). The variables with the highest contributions were Precipitation Warmest Quarter (35.6%), Mean Diurnal Range (23.4%), and Temperature Seasonality (14.3%). For the jackknife test, Precipitation Warmest Quarter had the highest training gain and Mean Temperature Warmest Quarter had the largest decreases in gain when omitted.

## Discussion

The multilocus population genetic data provide evidence for at least three genetically distinct lineages of *P. noxius* from eastern Asia (Japan, Taiwan, Hong Kong, and Malaysia), western Oceania (Australia, Palau, Guam, Saipan, Yap, Pohnpei, and Kosrae)/Japan/Taiwan, and American Samoa. Our data further suggest that admixture or migration of genotypes between the eastern Asia and Pacific island populations has likely occurred, agreeing with previously published reports on *P. noxius* populations in Japan and Taiwan (Akiba et al. 2015; Chung et al. 2015). Further, the isolates from American Samoa are genetically distinct from other previously studied geographic populations. At the *tef1* locus, the American Samoa population appears more closely related to the western Oceania/Japan/Taiwan lineage.

Our phylogenetic results from the LSU and ITS regions highlight the polyphyletic evolutionary history of *Phellinus* spp. and suggest that *P. noxius* is

phylogenetically distinct from other species within the *Phellinus*, which concurs with the results of Zhou et al. (2018). Several studies have examined the phylogeny of *Phellinus* and the closely related genera *Fomitiporella*, *Fomitiporia*, *Fuscoporia*, *Hymenochaete*, *Inonotus*, *Onnia*, and *Porodaedalea* using the LSU, ITS, and/or protein-coding regions (Wagner and Fischer 2002; Jeong et al. 2005; Brazee and Lindner 2013; Brazee 2015; Cloete et al. 2016; De Campos-Santana et al. 2016). According to these previous studies, most species within *Phellinus* are monophyletic; however, molecular analyses highlight that reclassification of some taxa at the genus level may be warranted because historical species delineations relied on convergent morphological and/or physiological characters. Using a combined data set of the ITS and mitochondrial small subunit, Jeong et al. (2005) found 13 lineages/species within *Phellinus*, *Hymenochete*, and *Onnia*, suggesting that definitions of fungal species within the Hymenochaetales have yet to be resolved. Results from both phylogenetic analyses of LSU and ITS regions suggest that more taxonomic work is needed to verify whether *P. noxius* is a synonym for *Pyrrhoderma noxium*, as suggested by Zhou et al. (2018). Our data suggest that *P. noxius* is distinct from *Pyrroderma noxium*, but focused studies are needed to determine if *P. noxius* isolates from this study belong to the genus *Pyrroderma*. The limited DNA sequence data suggest that the *P. noxius* isolates from our study may represent one or more cryptic species, such as was found within *Coniferiporia sulphurascens* (Leal et al. 2019). Comparative genomic studies among *P. noxius* and closely related taxa within the Hymenochaetales were conducted (Chung et al. 2017); however, additional genomic sequencing of more isolates and species will better inform the correct taxonomy and placement of *P. noxius* isolates among other closely related species.

Our data suggest that considerable genetic variation exists among and within the identified *P. noxius* lineages. These results concur with Chung et al. (2017) who found high rates of genetic variation using whole-genome sequencing of isolates predominately from Japan and Taiwan. In our study, high nucleotide diversity was identified for two populations of *P. noxius* (Eastern Asia and Western Oceania/Japan/Taiwan). These rates were comparable to diversity rates observed for other fungal species, including *Cryptococcus neoformans* (Leffler et al. 2012) and *Porodaedalea* spp. found across northern North America (Brazee and Lindner 2013). *Porodaedalea* spp., phylogenetically related to *P. noxius*, had rates of nucleotide diversity that ranged from 0.002 at the LSU to 0.008 at the *tef1*, which were similar to rates observed for *P. noxius* at the same loci (0.003 and 0.008, respectively) (Brazee and Lindner 2013).

The varied genetic diversity among our populations, e.g., Eastern Asia and Western Oceania/Japan/Taiwan vs. American Samoa, is perhaps attributable to 1) a recent introduction into American Samoa with an associated genetic bottleneck; and/or 2) movement of hybridization between the Eastern Asia and Western Oceania/Japan/Taiwan populations. Our data show that isolates from Malaysia and Hong Kong were genetically distinct from isolates from the Pacific Islands and Australia. However, isolates from Japan and Taiwan were more similar, indicating possible genetic admixture of the two populations on Japan and Taiwan, but not in Malaysia nor Hong Kong. An earlier microsatellite study showed that the Ryukyu Islands and Ogasawara Islands in Japan (Akiba et al. 2015) each contained distinct populations of *P. noxius* with little evidence of gene flow between the two populations. It was further hypothesized that *P. noxius* on the Ogasawara Islands could have been introduced from Pacific Islands located to the East.

Results show that suitable climate spaces for combined genetic groups include areas in the southeastern United States (Florida), eastern Mexico, eastern Central America, northwestern and central eastern South America (e.g., Colombia, Ecuador, Peru, and Brazil), parts of Africa and Madagascar, eastern Asia, eastern Australia, and many of the Pacific Islands (Fig.6) . Though not analyzed for the American Samoa population alone because of the limited geographic distribution of occurrence points, suitable climate space is different for the eastern Asia and western Oceania/Japan/Taiwan lineages. For example, the eastern Asia lineage may pose a threat to northern Australia and many of the Pacific Islands, whereas the western Oceania/Japan/Taiwan lineage appears more suited for the climate space in eastern Australia, some of Pacific Islands, and areas of eastern Asia. However, our climate space models are based on currently available locations and climate variables. Increased sampling and changes in climate would likely affect projections of suitable climate space for the *P. noxius* populations.

A noteworthy result from this research is that Florida and the Hawaiian Islands are predicted to have a suitable

climate for *P. noxius*, though the pathogen has not been reported in either region (Fig. 6). The host range for *P. noxius* is very broad, with over 200 host species including fruit/nut crops, forest trees, and woody ornamental plants (Farr and Rossman 2019). Thus, *P. noxius* should be currently considered as an invasive threat to areas of North America and/or Hawaii. If changes in climate produce new geographic areas suitable for the pathogen in North America or other global regions, many woody species could be at risk.

Continued studies of the genetic diversity, population structure, evolution, reproductive system, and epidemiology of *P. noxius* are essential to understand the dispersal pathways for this destructive, invasive pathogen. Further surveys and collections in tropical areas including Vanuatu, Hainan China, New Caledonia, Fiji, French Polynesia, and Africa are needed to understand the full extent of this pathogen's invasiveness. Developing molecular tools to identify each distinct lineage described herein will help to determine the geographic distribution and host range of each lineage. Continued research of *P. noxius* populations will inform management strategies by better characterizing host range, suitable climate space, and potential/existing hybridization among *P. noxius* populations, which will contribute to improved predictions of geographic regions that are at risk of invasion. Further analyses are recommended to assess regional population structure, gene flow among populations, diversity in recently observed populations, and potential suitable climate space for specific genotypes. Understanding long-distance dispersal mechanisms of the pathogen will help determine potential pathways of spread, so that measures can be implemented to limit invasive movement of *P. noxius*.

**Acknowledgements** The authors thank Hsin-Han Lee, Yu-Ching Huang, Ruey-Fen Liou (Taiwan); Regent Y. C. Lam, Mike W.K. Leung, L.M. Chu, H.S. Kwan (Hong Kong); Zakaria Yusof, Noraini Sikin Yahya and Mohd Fakaruddin Baharudin (Malaysia); and Ashley Lehman (USDA Forest Service, Pacific Northwest Research Station, Resource Monitoring and Assessment) for contributing *P. noxius* isolates and expertise. In addition, the authors thank the following for their professional assistance in the collection of *P. noxius*: Roger Brown, Sheeka Teryama, Joe Afaisen, Ruddy Estoy, Roland Quitugua, James McConnell, John Horeg, Mario Martinez (Guam); Vic Guerrero, Manny Tenorio, Arnold Route (Saipan); Arlene Rosenkrans, Gibson Santos, Rodasio Samuel, Konrad Engleberger (Pohnpei); Blair Charley, Maxson Nithan, Katie Friday, Erick Waguk (Kosrae); and Francis Ruegorong, Margie Falanruw (Yap). This work is supported by in part RREA grant no. NI18RREAFXXXG016 from the USDA National Institute of Food and Agriculture, USDA Forest Service (FS), Forest Health Protection (FHP) Special Technology Development Program (STDP-R5-2015-01 and STDP-R5-2019-02), and USDA FS, FHP, Region 5, and by the College of Agricultural Sciences, Colorado State University.

**Compliance with ethical standards**

**Conflict of interest** All authors declare that they have no potential sources of conflict of interest.

**Human and animals rights** Current research does not involve human participants or animals.

**Informed consent** All authors have been personally and actively involved in substantive work leading to the manuscript, and will hold themselves jointly and individually responsible for its content All authors reviewed the manuscript and agree to submit it in the present form.

## References

Akiba, M., Ota, Y., Tsai, I. J., Hattori, T., Sahashi, N., & Kikuchi, T. (2015). Genetic differentiation and spatial structure of *Phellinus noxius*, the causal agent of brown root rot of woody plants in Japan. *PLoS One, 10*(10), e0141792. https://doi.org/10.1371/journal.pone.0141792.

Ann, P.-J., Chang, T.-T., & Ko, W.-H. (2002). *Phellinus noxius* brown root of fruit and ornamental trees in Taiwan. *Plant Disease, 86*, 820–826.

Araújo, M. B., Pearson, R. G., Thuiller, W., & Erhard, M. (2005). Validation of species–climate impact models under climate change. *Global Change Biology, 11*, 1504–1513.

Bickford, D., Lohman, D. J., Sodhi, N. S., Ng, P. K. L., Meier, R., Winker, K., et al. (2007). Cryptic species as a window on diversity and conservation. *Trends in Ecology & Evolution, 22*, 148–155.

Brasier, C. M. (2001). Rapid evolution of introduced plant pathogens via interspecific hybridization: Hybridization is leading to rapid evolution of Dutch elm disease and other fungal plant pathogens. *BioScience, 51*, 123–133.

Brazee, N. J. (2015). Phylogenetic relationships among species of *Phellinus sensu stricto*, cause of white trunk rot of hardwoods from northern North America. *Forests, 6*, 4191–4211.

Brazee, N. J., & Lindner, D. L. (2013). Unraveling the *Phellinus pini* s.l. complex in North America: A multilocus phylogeny and differentiation analysis of *Porodaedalea*. *Forest Pathology, 43*, 132–143.

Brooks, F. (2002a). Brown root rot disease in American Samoa's tropical rain forests. *Pacific Science, 56*, 377–387.

Brooks, F. (2002b). Brown root rot. *The Plant Health Instructor.* https://doi.org/10.1094/PHI-I-2002-0923-01(Updated2013).

Chakroaborty, S. (2013). Migrate or evolve: Options for plant pathogens under climate change. *Global Change Biology, 19*, 1985–2000.

Chang, T.-T. (1996). Survival of *Phellinus noxius* in soil and in the roots of dead host plants. *Phytopathology, 86*, 272–276.

Chung, C.-L., Huang, S.-Y., Huang, Y.-C., Tzean, S.-S., Ann, P.-J., Tsai, J.-N., et al. (2015). The genetic structure of *Phellinus noxius* and dissemination pattern of brown root rot disease in Taiwan. *PLoS One, 10*(10), e0139445.

Chung, C.-L., Lee, T. J., Akiba, M., Lee, H. H., Kuo, T. H., Liu, D., et al. (2017). Comparative and population genomic landscape of *Phellinus noxius*: A hypervariable fungus causing root rot in trees. *Molecular Ecology, 26*, 6301–6316.

Clement, M., Posada, D., & Crandall, K. A. (2000). TCS: a computer program to estimate gene genealogies. *Molecular Ecology, 9*, 1657–1660.

Cloete, M., Fischer, M., De Plessis, I. L., Mostert, L., & Halleen, F. (2016). A new species of *Phellinus sensu stricto* associated with esca on grapevine in South Africa. *Mycological Progress, 15*, 25.

Corner, E. J. H. (1932). The identification of the brown root fungus. *Gardeners Bulletin Straits Settlements, 5*, 317–350.

Cunningham, G. H. (1965). Polyporaceae of New Zealand. *Bulletin of the New Zealand Department of Industrial Research, 164*, 221–222.

De Campos-Santana, M., Amalfi, M., Castillo, G., & Decock, C. (2016). Multilocus, DNA-based phylogenetic analyses reveal three new species lineages in the *Phellinus gabonensis-P. caribaeo-quericola* species complex, including *P. amazonicus* sp. nov. *Mycologia, 106*, 939–953.

Dean, M. D., & Ballard, J. W. O. (2004). Linking phylogenetics with population genetics to reconstruct the geographic origin of a species. *Molecular Phylogenetics and Evolution, 32*, 998–1009.

Desperez-Loustau, M.-L., Robin, C., Buée, M., Courtecuisse, R., Garbeye, J., Suffert, F., et al. (2007). The fungal dimension of biological invasions. *Trends in Ecology & Evolution, 22*, 472–480.

Dlugosch, K. M., & Parker, I. M. (2008). Founding events in species invasions: Genetic variation, adaptive evolution, and the role of multiple introductions. *Molecular Ecology, 17*, 431–449.

Drummond, A. J., Suchard, M. A., Xie, D., & Rambaut, A. (2012). Bayesian phylogenetics with BEAUti and the BEAST 1.7. *Molecular Biology and Evolution, 29*, 1969–1973.

Edgar, R. C. (2004) MUSCLE: multiple sequence alignment with high accuracy and high throughput. *Nucleic Acids Resesearch,* 32, 1792–1797.

Elith, J., Graham, C. H., Anderson, R. P., Dudík, M., Ferrier, S., Guisan, A., et al. (2006). Novel methods improve prediction of species' distributions from occurrence data. *Ecography, 29*, 129–151.

Elith, J., Phillips, S. J., Hastie, T., Dudík, M., Chee, Y. E., & Yates, C. J. (2011). A statistical explanation of MaxEnt for ecologists. *Diversity and Distributions, 17*, 43–57.

Farr, D. F., & Rossman, A. Y. (2019). Fungal Databases, U.S. National Fungus Collections, ARS, USDA. Retrieved September 9, from https://nt.ars-grin.gov/fungaldatabases/

Fischer, M. C., Henk, D. A., Briggs, C. J., Brownstein, J. S., Madoff, L. C., McCraw, S. L., & Gurr, S. J. (2012). Emerging fungal threats to animal, plant and ecosystem health. *Nature., 484*, 186–194.

Forsman, A. (2014). Effects of genotypic and phenotypic variation on establishment are important for conservation, invasion, and infection biology. *Proceedings of the National Academy of Sciences (USA)*, 111, 302–307.

Grünwald, N. J., & Goss, E. M. (2011). Evolution and population genetics of exotic and re-emerging pathogens: Novel tools and approaches. *Annual Review of Phytopathology, 49*, 249–267.

Guindon, S., Dufayard, J., Lefort, V., Anisimova, M., Hordijk, W., & Gascuel, O. (2010). New algorithms and methods to estimate maximum-likelihood phylogenies: Assessing the performance of PhyML 3.0. *Systematic Biology, 59*, 307–321.

Heled, J. & Drummond, A.J. (2010) Bayesian inference of species trees from multilocus data. *Molecular Biology and Evolution*, 27, 570–580.

Hodges, C. S., & Tenorio, J. A. (1984). Root disease of *Delonix regia* and associated tree species in the Mariana Islands caused by *Phellinus noxius*. *Plant Disease, 68*, 334–336.

Hudson, R. R., Boos, D. D., & Kaplan, N. L. (1992a). A statistical test for detecting population subdivision. *Molecular Biology and Evolution, 9*, 138–151.

Hudson, R. R., Slatkin, M., & Maddison, W. P. (1992b). Estimates of levels of gene flow from DNA sequence data. *Genetics, 132*, 583–589.

Jeong, W. J., Young, W. L., Jin, S. L., & Hack, S. J. (2005). Phylogeny of *Phellinus* and related genera inferred from combined data of the ITS and mitochondrial SSU rDNA sequences. *Journal of Microbiology and Biotechnology, 15*, 1028–1038.

Karger, D. N., Conrad, O., Böhner, J., Kawohl, T., Kreft, H., Soria-Auza, R. W., et al. (2017). Climatologies at high resolution for the earth land surface areas. *Scientific Data, 4*, 170122.

Leal, I., Bergeron, M.-J., Feau, N., Tsui, C. K. M., Foord, B., Pellow, K., Hamelin, R. C., & Sturrock, R. N. (2019). Cryptic speciation in western North America and eastern Eurasia of the pathogens responsible for laminated root rot. *Phytopathology, 109*, 456–468.

Leffler, E.M., Bullaughey, K., Matute, D.R., Meyer, W.K., Ségurel, L., Venkat, A., et al. (2012) Revisiting an old riddle: What determines genetic diversity levels within species? *PLoS Biology*, 10, e1001388.

Leibhold, A. M., Brockerhoff, E. G., Garrett, L. J., Parke, J. L., & Bitton, K. O. (2012). Live plant imports: The major pathway for forest insect and pathogen invasions of the US. *Frontiers in Ecology and the Environment, 10*, 135–143.

Kearse, M., Moir, R., Wilson, A., Stones-Havas, S., Sheung, M., Sturrock, S., et al. (2012) Geneious basic: An integrated and extendable desktop software platform for the organization and analysis of sequence data. Bioinformatics, 28, 1647–1649.

Matheny, P. B. (2005). Improving phylogenetic inference of mushrooms with RPB1 and RPB2 nucleotide sequences (*Inocybe*; Agaricales). *Molecular Phylogenetics and Evolution, 35*, 1–20.

Minin, V., Abdo, Z., Joyce, P., & Sullivan, J. (2003). Performance-based selection of likelihood models for phylogeny estimation. *Systematic Biology, 52*, 674–683.

Rambaut, A. (2009). FigTree v1.2.2. http://tree.bio.ed.ac.uk/software/figtree/. Accessed 26 Aug 2015

Rehner, S. A., & Buckley, E. (2005). A Beauveria phylogeny inferred from nuclear ITS and EF1-a sequences: Evidence for cryptic diversification and links to Cordyceps teleomorphs. *Mycologia, 97*, 84–98.

Rehner, S., & Samuels, G. (1994). Taxonomy and phylogeny of *Gliocladium* analyzed from nuclear large subunit ribosomal DNA sequences. *Mycological Research, 98*, 625–634.

Rozas, J. J., Sanchez-DelBarrio, J. C., Messeguer, X., & Rozas, R. (2003). DnaSP, DNA polymorphism analyses by the coalescent and other methods. *Bioinformatics, 19*, 2496–2497.

Tajima, F. (1989) Statistical methods for testing the neutral mutation hypothesis by DNA polymorphism. *Genetics*, 123, 585–595.

Vilgalys, R., & Hester, M. (1990). Rapid genetic identification and mapping of enzymatically amplified ribosomal DNA from several *Cryptococcus* species. *Journal of Bacteriology, 172*, 4238–4246.

Wagner, T., & Fischer, M. (2002). Proceeding towards a natural classification of the worldwide taxa *Phellinus* s.l. and *Ionotus* s.l., and phylogenetic relationships of allied genera. *Mycologia, 94*, 998–1016.

White, T. J., Bruns, T., Lee, S., & Taylor, J. (1990). Amplification and direct sequencing of fungal ribosomal RNA genes for phylogenetics. In N. Innis, D. Gelfand, J. Sninsky, & T. White (Eds.), *PCR protocols: A guide to methods and applications* (pp. 315–322). New York: Academic Press.

Zhou, L.-W., Ji, X.-H., Vlasák, J., & Dai, Y.-C. (2018). Taxonomy and phylogeny of *Pyrrhoderma*: A redefinition, the segregation of *Fulvoderma*, gen. nov. and identifying four new species. *Mycologia, 110*, 872–889.